GEP-NET: Acromegaly

8th POSTGRADUATE COURSE IN ENDOCRINE SURGERY

21 – 24 September 2006

Aghia Pelaghia- Heraklion, Crete, Greece

G.Tolis, ***MD, PhD, FRCP,CSPQ***

FELOWS OF THE DIVISION

G. Rombopoulos, E. Katounda, V. Kaltsidou, P. Xekouki, A. Lytras, D. Kaltsas, A. Protonotariou

Division of Endocrinology and Metabolism, Hippokrateion General Hospital, Athens

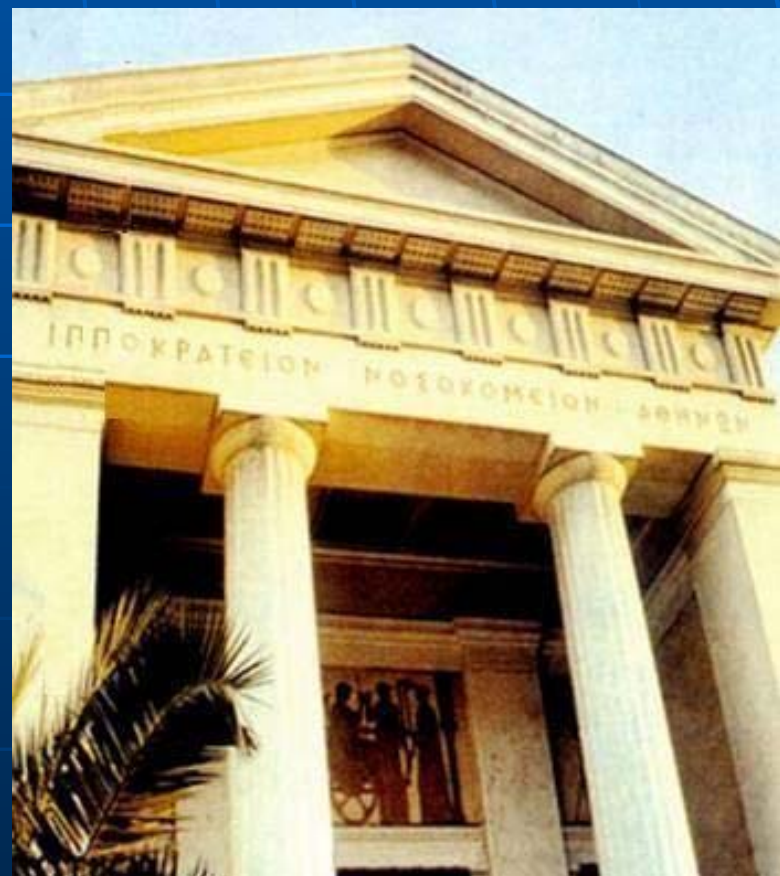

Acromegaly: Case report

- Classic acral and soft tissue features of acromegaly developed rapidly in a 63-year-old man.
- Serum GH levels were nonsuppressible *(OGTT, acute octreotide and not stimulated with GHRH)* and levels of plasma insulin-like growth factor-1 (IGF-1) were elevated.
- A computed tomography scan of the pituitary was normal.
- Search for ectopic source was initiated.

Shereen Ezzat, 1993

Ectopic Growth Hormone Gene Expression by a Metastatic Pancreatic Tumor

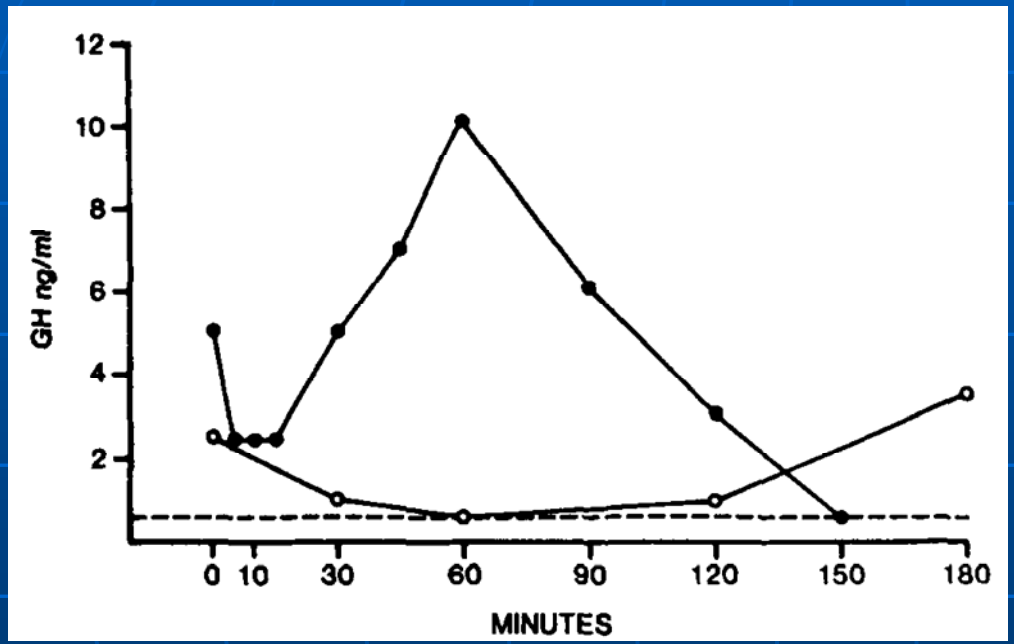

Figure 1. Response of GH to oral glucose (75 g) suppression (open circles) or intravenous GHRH,_4a (100 *fig)* stimulation (closed circles) **3 months after initial resection of an ectopic pancreatic tumor producing GH.** Glucose and GHRH were administered at 0 minutes on separate days.

- CT scan of the abdomen showed an 8.1 x 6.6 cm mass in the head of the pancreas. Surgical resection of this pancreatic tumor was followed by rapid normalization of GH levels.

Shereen Ezzat, 1993

Recurrent Acromegaly Resulting from Ectopic Growth Hormone Gene Expression by a Metastatic Pancreatic Tumor

One year later, acral enlargement, carpal tunnel compression, and abdominal distension recurred.

	Hormone				
	*GH** *(ng/ml)* *(< 2)†*	*IGF-1* *(U/ml)* *(0.3–1.9)*	*PRL* *(ng/ml)* *(3.0–14.7)*	*T4* *(μg/dl)* *(4.3–9.1)*	*FPG‡* *(mg/dl)* *(70–110)*
Diagnosis					
Initial	25	2.8	11	9.4	76
Postoperative	1.4	1.2			100
Recurrence					
Early	36	4.6	16	8.8	116
Late	910	9.5	16		156

FPG: fasting plasma glucose; PRL: prolactin; GH: growth hormone; IGF: insulin-like growth factor.

* Nadir value after glucose load.

† Normal value or range.

‡ Fasting plasma glucose.

Table 1. Hormone and metabolic profile during the different clinical stages of recurrent ectopic growth hormone-producing pancreatic tumor.

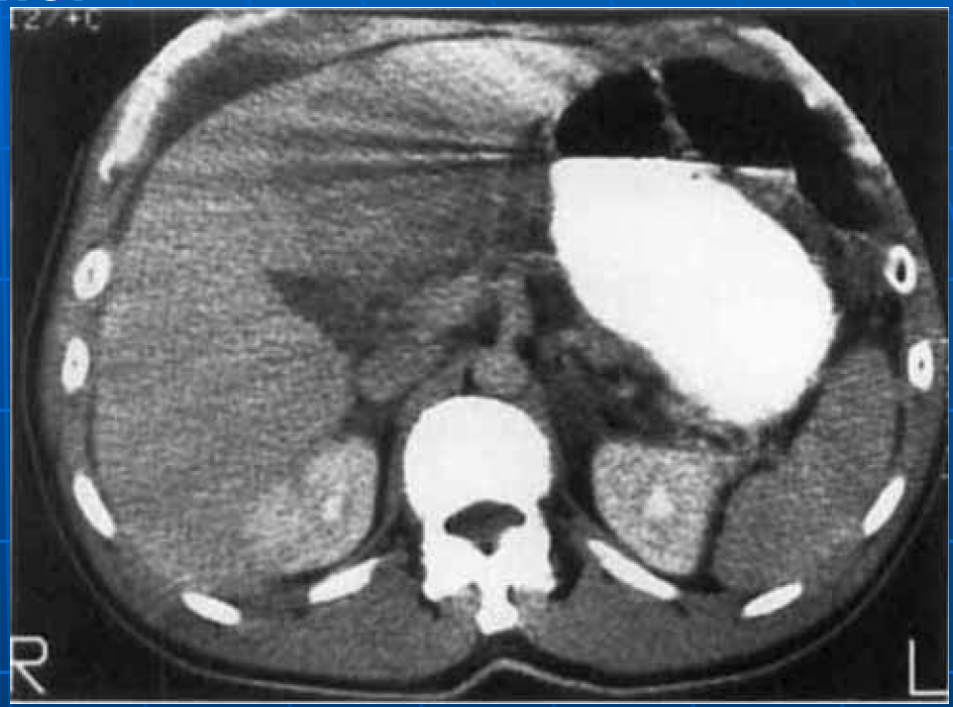

Figure 2. Computed tomography scan of the abdomen 1 year after initial surgery showing multiple intraperitoneal masses among the loops of the bowel, a 7-cm density in the left lobe of the liver, and ascites.

Shereen Ezzat, 1993

SUCCESSFUL TREATMENT OF ACROMEGALY BY REMOVAL OF A TUMOR

- A 21-yr-old woman with Turner's syndrome presented with signs and symptoms of acromegaly. The serum growth hormone (GH) (95±9.4 ng/ ml; mean±SEM) and somatomedin C (11 U/ml) levels were elevated, and an increase in GH levels after glucose instead of normal suppression.
- The pituitary fossa volume was greater than normal (1,440 mm3) and the presence of a pituitary tumor was assumed.
- The patient underwent transsphenoidal surgery and a large "tumor" was identified and removed. The patient made an uneventful recovery, *but serum GH and somatomedin C levels remained elevated.*
- *The path report indicated GH hyperplasia*

M. Thorner, 1982

SUCCESSFUL TREATMENT OF ACROMEGALY BY REMOVAL OF A PANCREATIC ISLET TUMOR **SECRETING GHRH**

- A CT scan of the abdomen showed a 5-cm diam mass with capsular calcification in the tail of the pancreas.
- At laparotomy a 55-g tumor was excised from the tail of the pancreas. There was no evidence for tumor extension or for metastases. The patient recovered postoperatively with resolution of acromegaly by both clinical and biochemical criteria.

M. Thorner, 1982

Acromegaly with no Evidence of MEN1

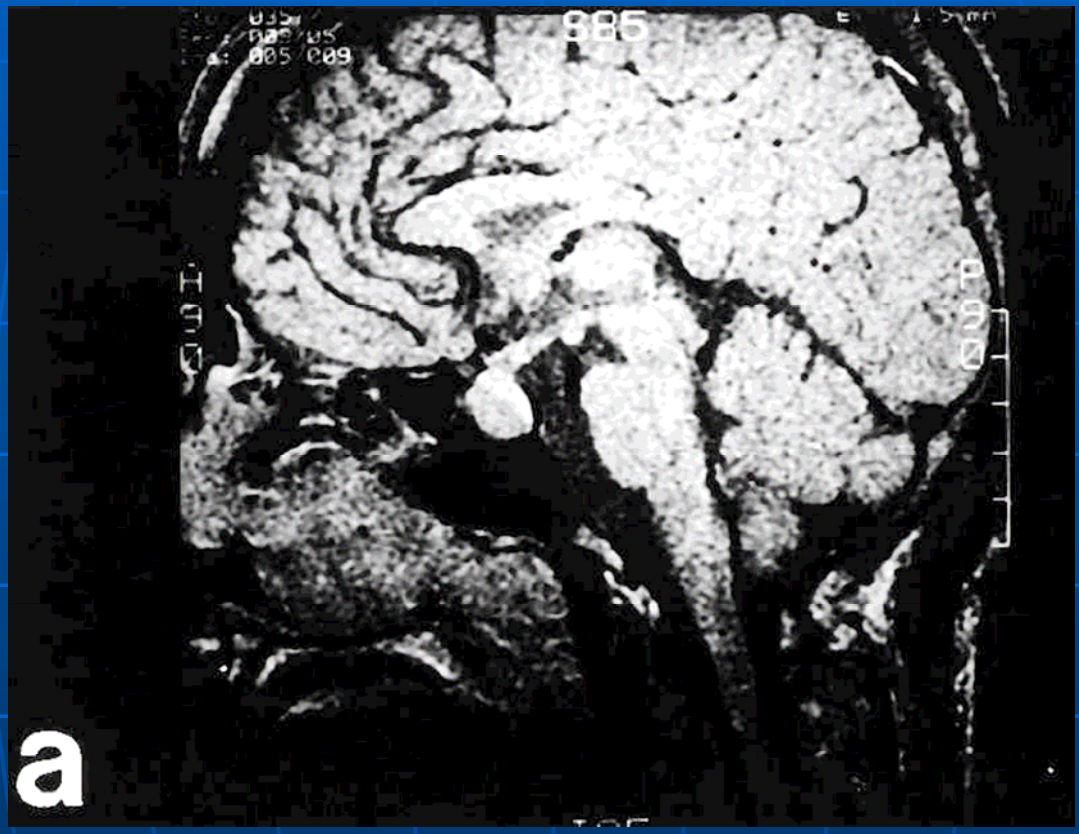

Fig 2. Brain MRI imaging

- A 48-year-old male was diagnosed as having acromegaly and a pituitary tumor was discovered by head computerized tomography.

S. KAWA, 1997

Growth Hormone-Releasing Hormone Producing Pancreatic Tumor with No Evidence of MEN1

An abdominal CT scan showed a large mass of 85 x 65 x 80 mm involving the pancreatic tail, which was highly enhanced with contrast medium.

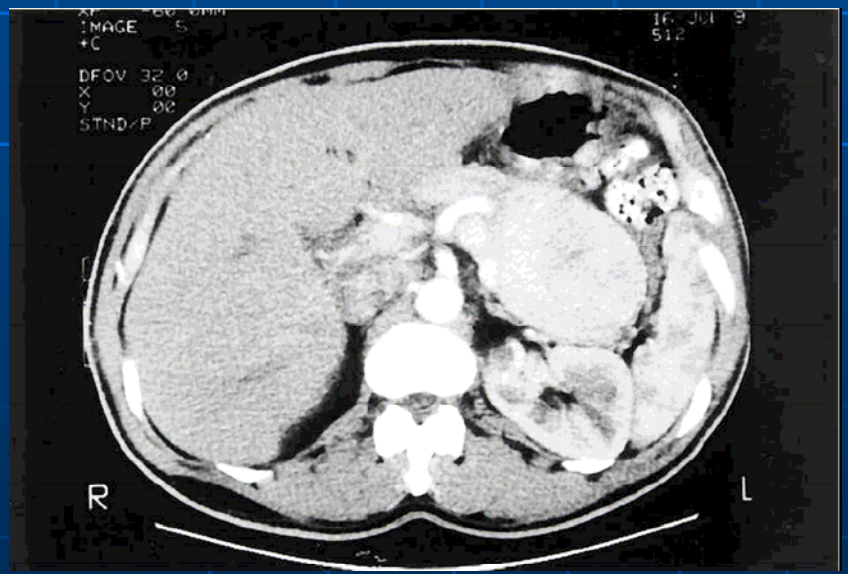

Fig 4. Percutanaeous transhepatic portal venous sampling. GRH level increases at the tumor region of the splenic vein. The step-up ratio at this point was 144%, indicating that GRH was actively produced by the tumor. SVC: superior vena cava, IVC: inferior vena cava, PV: portal vein, SMV: supramesenteric vein, SPV: splenic vein.

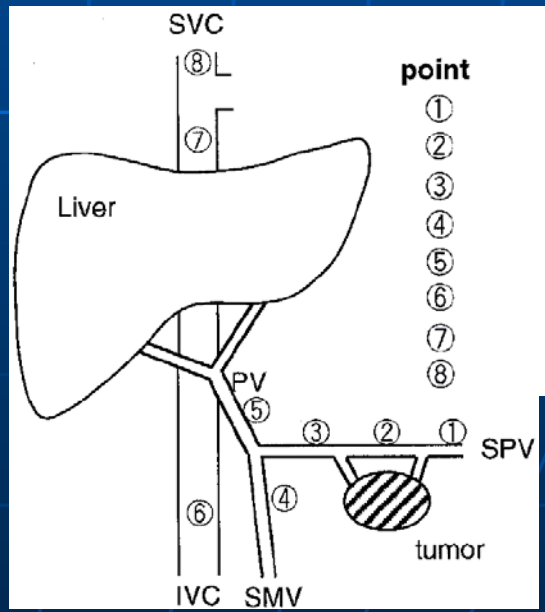

point	GRH (pg/ml)	Step up ratio (%)
①	94850	144
②	57910	49
③	50920	31
④	47260	21
⑤	45260	16
⑥	38940	0
⑦	43260	11
⑧	41600	7

S. KAWA, 1997

Growth Hormone-Releasing Hormone Producing Pancreatic Tumor with No Evidence of MEN1

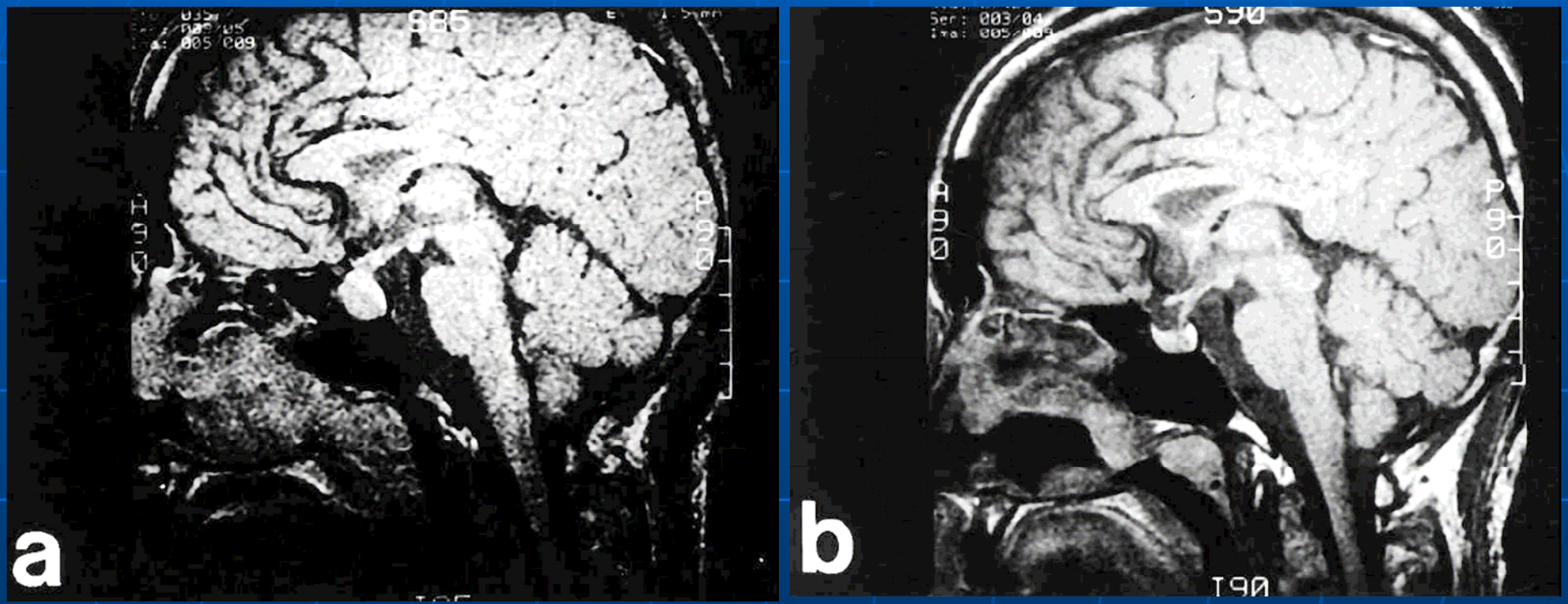

Fig 2. Brain MRI imaging: (a) before operation for pancreatic endocrine tumor, (b) one year after operation. Significant reduction of pituitary size is seen after the operation.

S. KAWA, 1997

Ectopic secretion of GHRH by GEP-NET tumors

- The association of acromegaly by GEP-NET tumors had been widely recognized in several patients prior to the characterization of hypothalamic GHRH Carcinoid tumors comprise most of the tumors associated with ectopic GHRH secretion, the majority bronchial in origin.
- Pancreatic cell tumors, small-cell lung cancers, adrenal adenoma, pheochromocytoma, medullary thyroid, endometrial and breast cancer have also rarely been described to express GHRH and cause acromegaly.

M. Doga, 2001

Ga-Octreotide-PET in neuroendocrine tumors a comparison with In-Octreoscan

Ga-octreotide-PET might be an effective method in the detection of neuroendncrine tumors with expression of somatostatin receptors. It could be also useful in selection of patients for somatostatin analogue treatment. Although a larger number of patients is needed, based on our own preliminary observations, Ga-octreotide-PET may be the technique of choice in relation to "'In-octretnide scintigraphy because can offer several potential advantages: a better imaging quality with a better resolution for visualization and detection of lesions, the shorter half life of Ga allows administration of much larger tracer doses with no additional radiation exposure, the residual activity within the patient is very low two hours after examination, obviating concerns of exposure to families or staff to incidental radiation. and finally, the investigation can be performed in the same day, avoiding hospitalisation or further inconveniences to the patient.

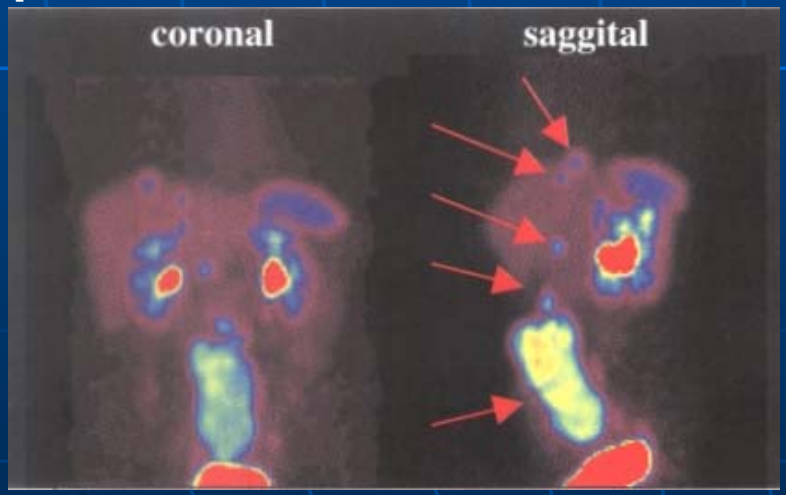

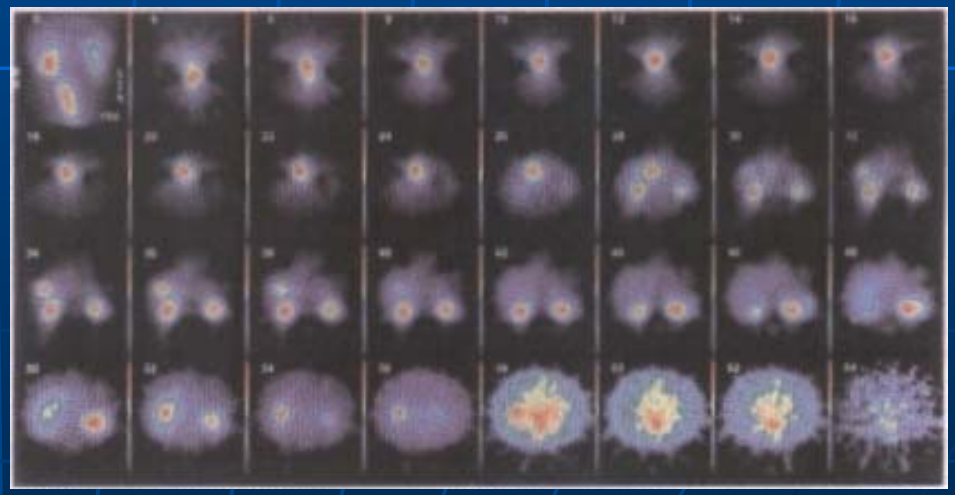

Figure 1. Patient with carcinoid tumor and suspicion of metastatic disease. Ga-octreotide-PET(left) and In-octreotide tomographic scintigraphy (right) show multiple metastases.

"C-Metomidate -PET in diagnosis of adrenocortical tumors

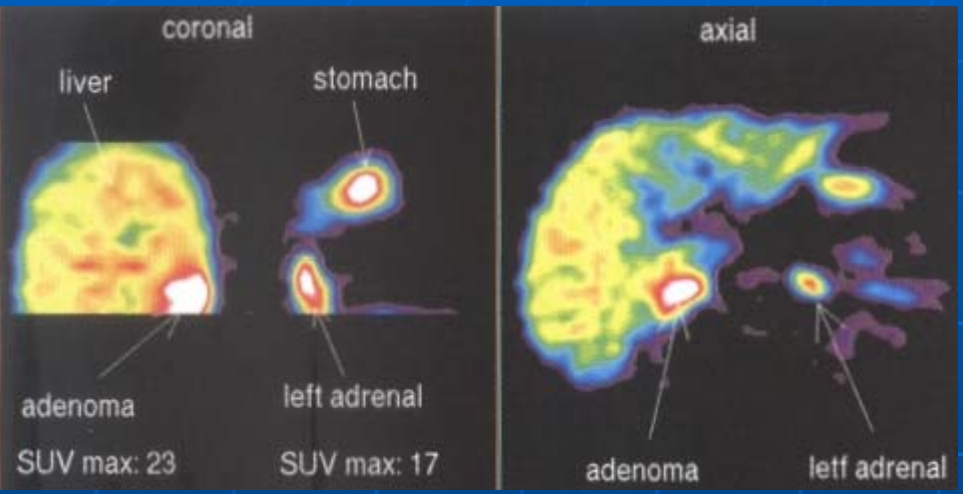

Figure 1. Adrenocortical adenoma in the right side. Elevated and homogeneous MTO uptake.

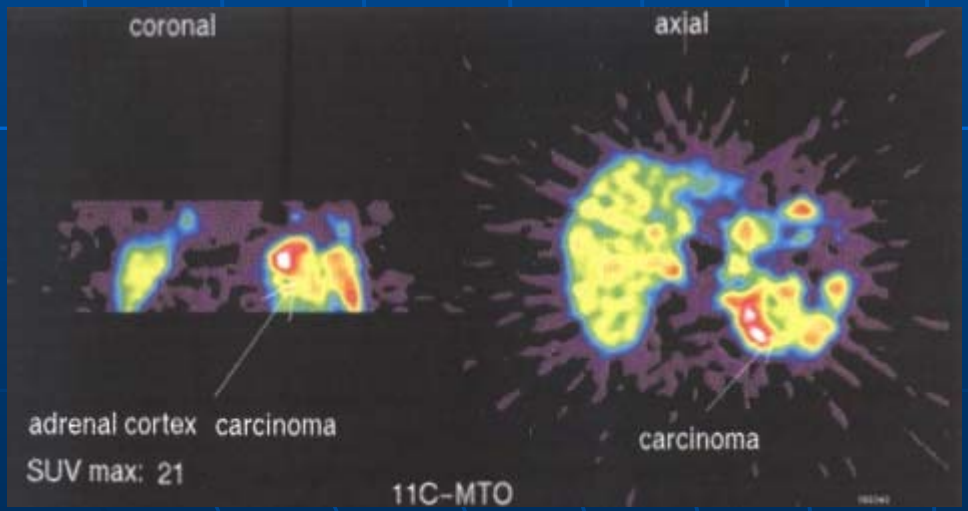

Figure 2. Carcinoma adrenal in the left side. Large mass with high and irregular MTO uptake as well as areas with lack of activity suggestive of necrosis.

Conclusions

"C-metomidate-PET (MTO-PET) provides an excellent visualization of adrenal tumors coming from the adrenal cortex, mostly adenomas, allowing α correct discrimination of lesions from adrenal cortical origin from non-cortical lesions.

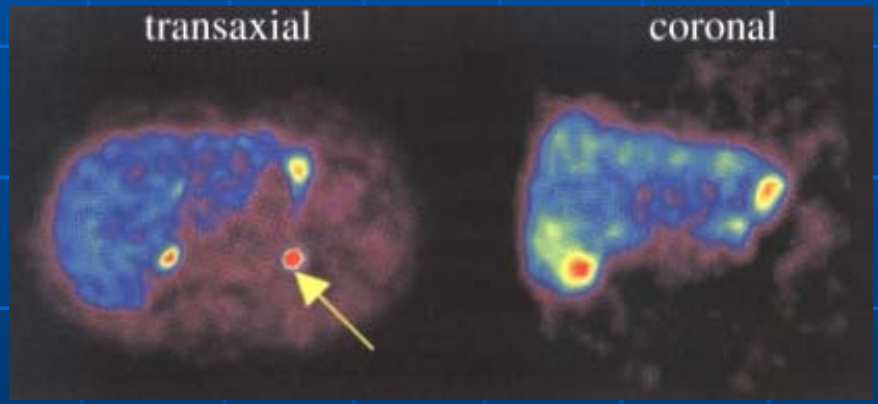

Figure 3. Patient with recurrent left adrenal carcinoma (left, yellow arrow) and liver metastases (right).

"C-Hydroxyephedrine-PET (HED-PET) in assessment of pheochromocytoma

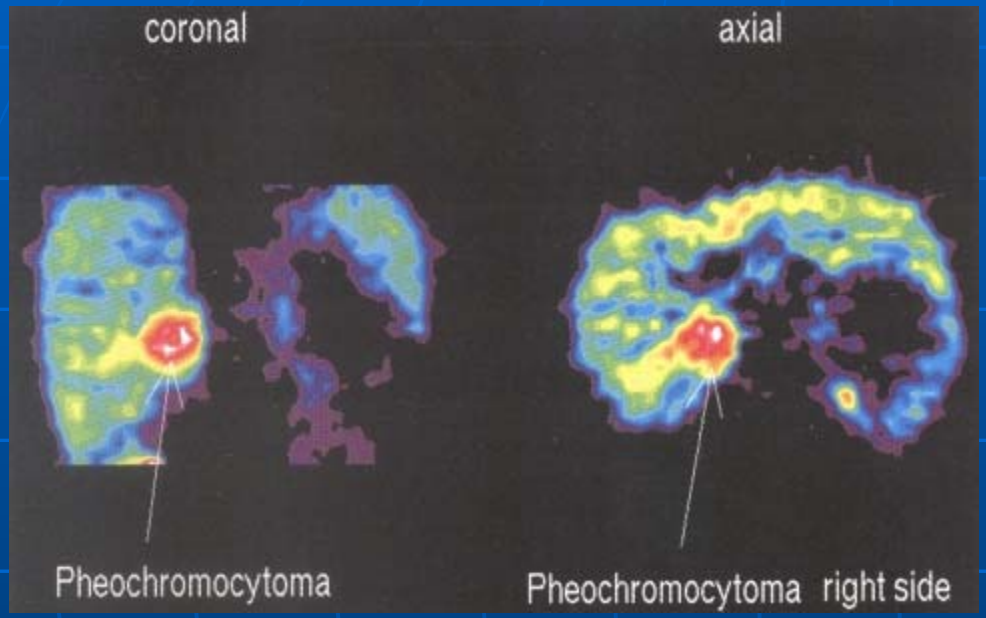

Figure 1. 1. Pheochromocytoma in the right adrenal gland.

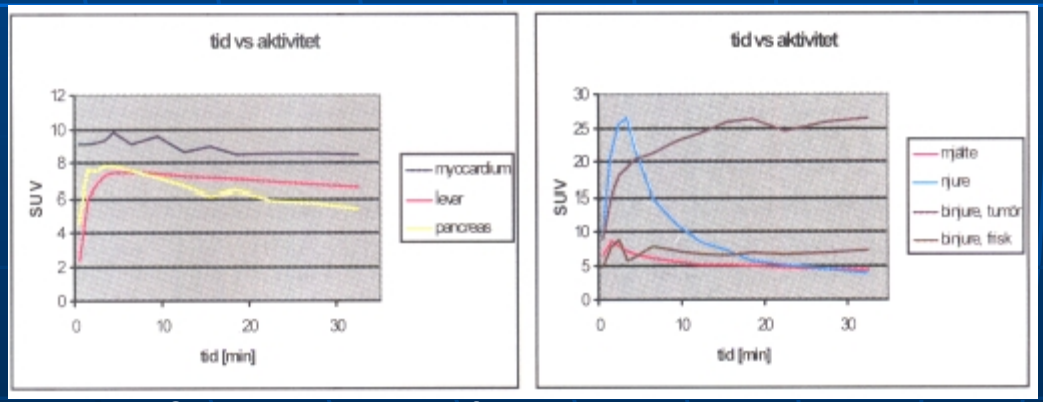

Figure 2. Curves time-activity of myocardium, liver and pancreas (left) and tumor, normal adrenal, spleen and kidney (right).

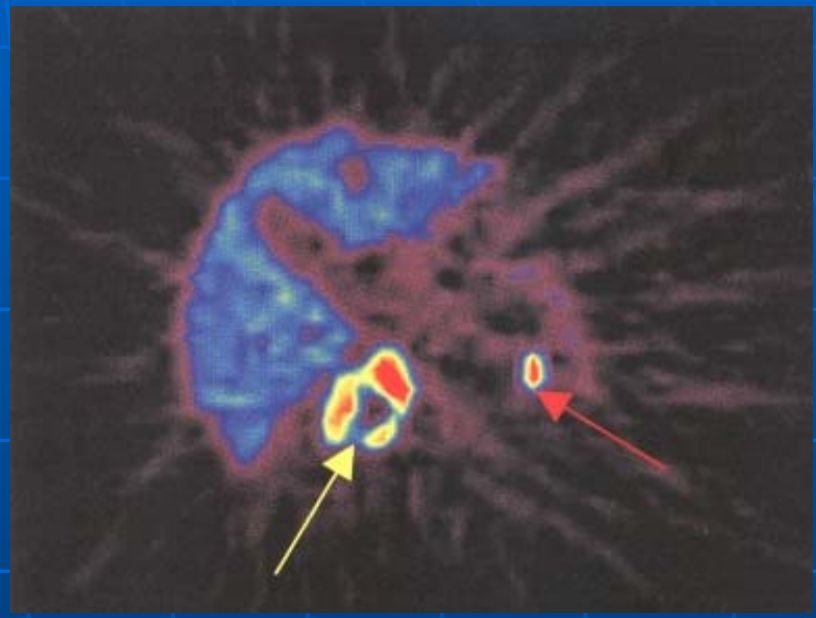

Figure 3. Necrotic pheochromocytoma in the right adrenal gland (yellow arrow). Normal uptake in the left one (red arrow).

Conclusions

HED-PET is α non-invasive technique very useful in the management of pheochromocytomas. HED-PET detects and localizes this kind of tumor with high accuracy, providing high quality functional images.

MET-PET of parathyroid tissue in hyperparathyroidism - preoperative localisation and tracer accumulation

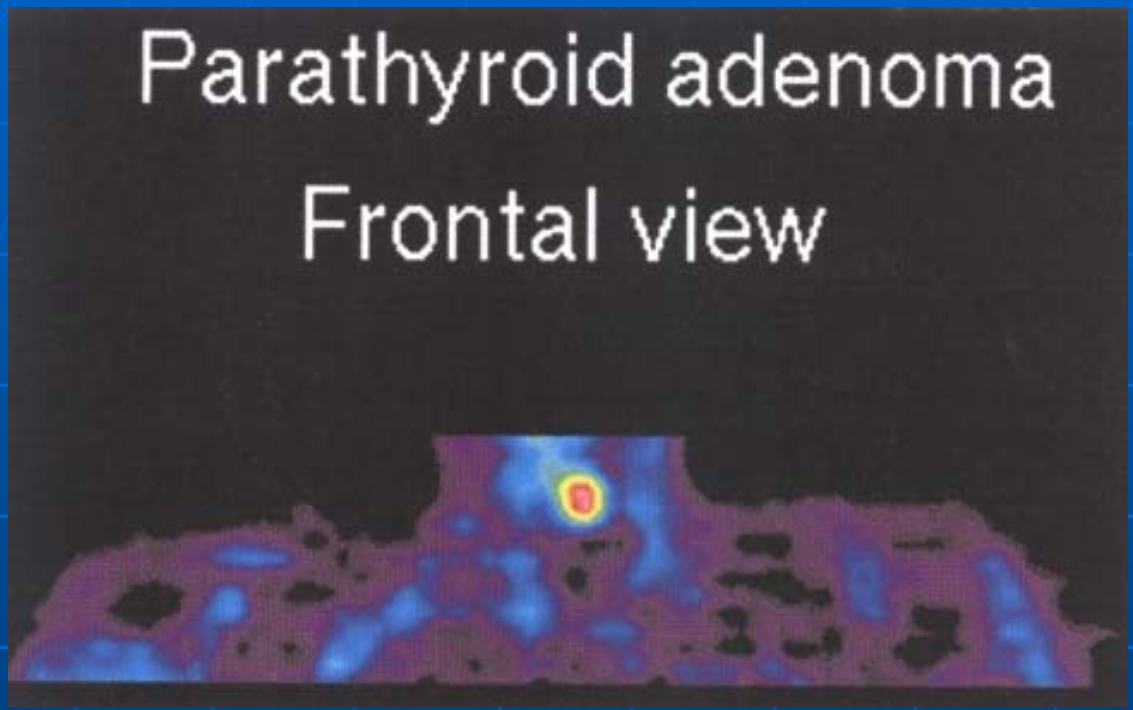

MET- PET offers promising potential in the preoperative localisation and metabolic characterisation of abnormal parathyroid tissue in patients with hyperparathyroidism.

Following surgery of the neck for thyroid or parathyroid disease the normal anatomy and fasciae planes are obscured. In the reoperative patient with hyperparathyroidism (HPT) preoperative localisation of the enlarged hyperparathyroid tissue is therefore important for the success of repeated surgery.

The rationale for the study was to evaluate preoperative localisation utilising PET with L-[methyl- C]methionine (MET) in comparison to computed tomography (CT) and ultrasound (US) and to characterise MET accumulation in the different histopathological parathyroid tissue subgroups in correlation with biochemical parameters.

Altogether 34 patients with primary (η=32) or secondary HPT were investigated with positron emission tomography prior to primary or reoperative (η=25) parathyroid surgery. A dynamic scanning sequence was started in connection with intravenous administration of 750 MBq of MET using α Scanditronix GE4096 wholebody camera. Data from 14 to 45 minutes were summated to images of radioactivity distribution. Parathyroid METaccumulation was analysed for integrated uptake values in defined tissue volumes standardised for the injected dose and body weight (SUV), 4 contiguous pixels of maximal accumulation (SUVhs), SUV multiplied by area of region of interest (SUVr) and the excised tissue weight (SUVw). Transport rate constants (slope, slope hs) were calculated according to Patlak using plasma C-activity corrected for MET-metabolites. Intravenously contrast- enhanced CT (η=29) was performed on α Siemens Somatom Plus scanner using 4 mm slice thickness and increment. **US** (η=29) utilised Acuson 128 equipped with α 5 or 7.5 MHz linear transducer.

Positron emission tomography in the management of carcinoid tumours

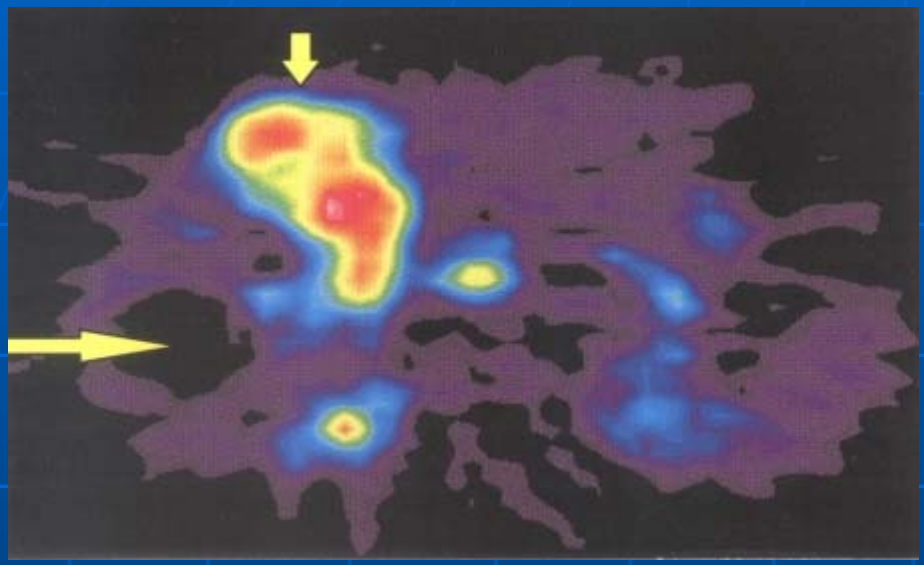

Figure 1. HTP-PET clearly demonstrating the high tracer accumulation in α minor part of the liver (short arrow), which by CT appeared to be almost totally replaced by tumour. The absence of tracer uptake in the tumour necrosis is also evident (long arrow).

- Conclusion
- ''C-5-HTP-PET provides novel possibilities for diagnosis as well as therapy monitoring in the management of patients with carcinoid tumours

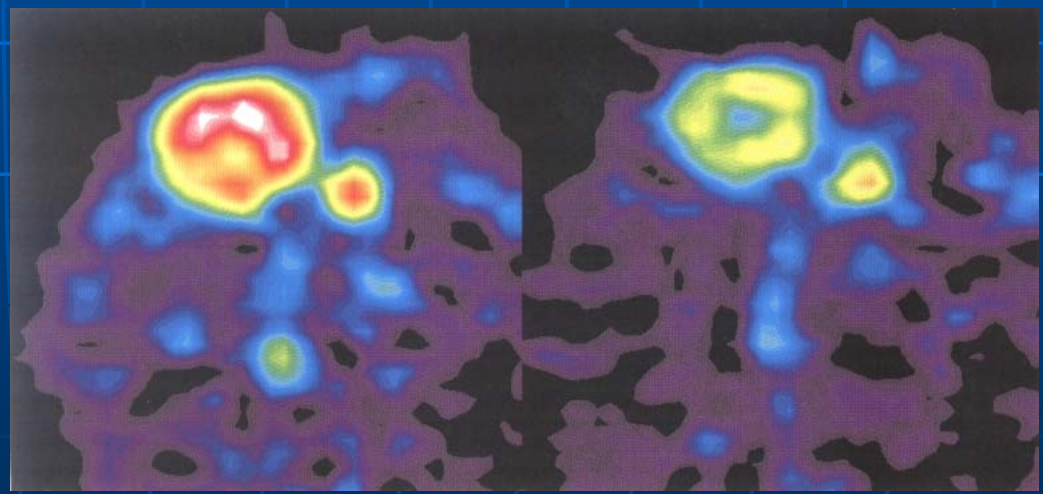

Figure 2. SUV images showing carcinoid liver metastases in the ventral part of the right liver lobe before and 3 months after start of medical therapy. The decrease in HTP tumour accumulation is evident.

In vivo demonstration of AADC-enzyme activity in endocrine pancreatic tumours

- Conclusions
- This study shows that using selective position labelling, in vivo enzymatic activity can be observed with PET and that significant decarboxylation occurs in the tested endocrine pancreatic tumours. Also, marked retention of radioactivity occurs after treatment with α somatostatin analogue.

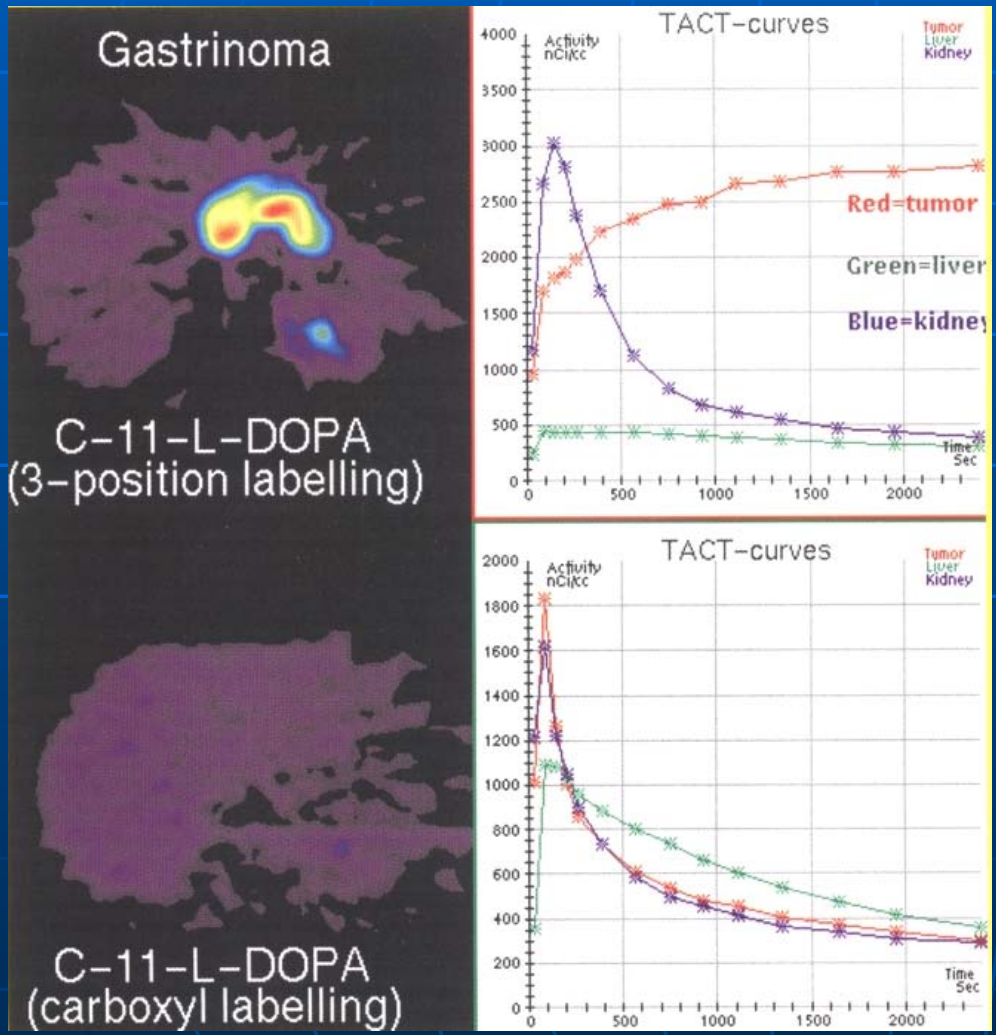

Figure. Two examinations of the same anatomical position of α patient with α pancreatic glucagonoma. Images are presented as average images of data 14-45 min. after tracer injection. At the first examination using DOP (top), the tracer accumulation in the tumour is easily appreciable whereas the DOC (bottom) fails to visualise the tumour, since the label follows the excreted CO,.

Characterisation of MAO-A expression in neuroendocrine gastrointestinal tumors and visualisation by PET

- Conclusions
- The study demonstrated that neuroendocrine gastrointestinal tumors are characterized by α high expression of MAO-A which can be assessed both in vitro and in clinical visualization by ''C-harmine (HAR)-PET. These findings add to the similarities between neurons and neuroendocrine tissue and indicate α possible future clinical application of HAR-PET in the management of neuroendocrine gastrointestinal tumors.

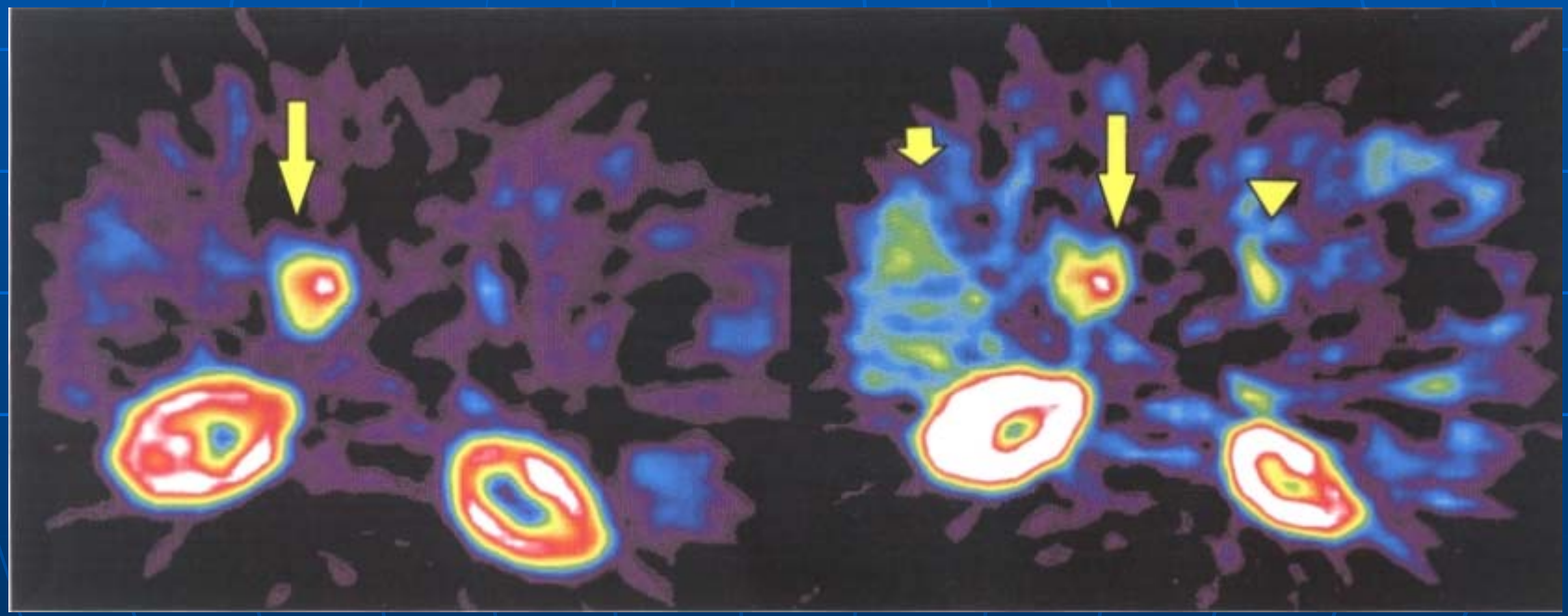

Figure. PET-visualisation using the "C-label led MAO-A tracer HAR with radioactivity distribution images 1-11 min. (left) and 15-45 min. (right) post injection. An insulinoma (arrow) is located in the head of the pancreas. At the latter time point compared to the early imaging phase, the tracer uptake, relative to tumor tissue, is higher in the liver (short arrow) and intestine (arrow head). λ high Uptake is also noted in the kidneys in both images.